Inorganica Chimica Acta 508 (2020) 119639

Contents lists available at ScienceDirect

Inorganica Chimica Acta

journal homepage: www.elsevier.com/locate/ica

Research paper

Synthesis, crystal structures, catalytic application and antibacterial activities of Cu(II) and Zn(II) complexes bearing salicylaldehyde-imine ligands

Chao Liu*, Ming-Xing Chen, Ming Li

School of Chemistry and Chemical Engineering, Suzhou University, Suzhou 234000, China

ARTICLE INFO

Keywords:
Cu(II) complex
Zn(II) complex
Crystal structure
Catalytic application
Antibacterial activity

ABSTRACT

Three novel copper(II) and zinc(II) complexes based on salicylaldehyde-imine ligands, namely [Cu(HL1)(CH_3CH_2OH)]·(CH_3COO) (**1**), [Zn_3(HL1)$_2$(CH_3COO)$_4$] (**2**), and [Zn_2(L2)]·(CH_3COO) (**3**) [H_2L1 = *N,N′*-bis(salicylidene)diethylenetriamine and H_3L2 = 2,2′-(1*E*,1′*E*)-(2,2′-(2-(2-hydroxyphenyl)imidazolidine-1,3-diyl)bis(ethane-2,1-diyl))bis(azan-1-yl-1-ylidene)bis(methan-1-yl-1-ylidene)diphenol] have been synthesized. The complexes were characterized by IR, melting point, and elemental analyses, and the crystal structures were further determined by single crystal X-ray diffraction. These three complexes demonstrated excellent catalytic activities in the decomposition reaction of H_2O_2, and the decomposition percent of the H_2O_2 ranged from 89% to 98% under the optimized reaction conditions. Additionally, the compounds were screened as antibacterial agents against three gram-negative bacteria (*Escherichia coli*, *Klebsiella pneumoniae* and *Pseudomonas aeruginosa*) and three gram-positive bacteria (*Bacillus subtilis*, *Staphylococcus aureus* and *Corynebacterium xerosis*). The results showed that complex **2** possessed stronger antibacterial activities than the two ligands and other two complexes.

1. Introduction

Nowadays, transition metal complexes have gained considerable attention on basis of their potential applications in catalytic fields [1–4]. In consideration of the concepts of green chemistry and the demands of chemical production, it has an extremely important practical significance to develop economic, efficient and low toxic transition metal complexes as catalyst [5,6]. Copper and zinc complexes display encouraging characteristics mentioned above and can catalyze various organic synthesis reactions [7,8]. As a typical sterilization disinfectant and bleaching agent, hydrogen peroxide was widely used in various aspects of industrial production and daily life, which caused serious water pollution yet [9]. Copper and zinc complexes as well as inorganic metal salt and metal oxide, possess application potentials in terms of catalyzing the decomposition reaction of hydrogen peroxide [10–13]. In addition, they also play important roles in the development of broad-spectrum biological agents including antibacterial, anticancer, antitumor, etc. [14–16].

It is well known that the construction of functional complexes is mostly attributed to functional attributes and structural characteristics of the ligands [2,3,15,16]. Consequently, considerable research attention has been focused on the design and synthesis of the suitable ligand. Owing to their stable structures, various coordination modes and strong coordination abilities, salicylaldehyde-imines are very effective chelating agents which can coordinate to transition metal ions, forming various mononuclear, binuclear, and multinuclear complexes with fascinating structures and interesting properties [17–24]. These findings will contribute to further researching of transition metal complexes bearing salicylaldehyde-imine ligands as catalyst or bioactivity agent. It is known that some complexes bearing salicylaldehyde-imine ligands show excellent catalytic activities, and others exhibit good biological activities [25,26]. However, as far as we know, the synthesis and application of the complexes with both catalytic activities and biological activities have rarely been reported.

Therefore, three novel copper(II) and zinc(II) complexes bearing salicylaldehyde-imine ligands (H_2L1 and H_3L2) have been synthesized by the condensation reactions of salicylaldehyde with diethylenetriamine and triethylenetetramine. The complexes have been characterized by various detection techniques and their structures have been determined by single crystal X-ray diffraction. [Cu(HL1)(CH_3CH_2OH)]·(CH_3COO) exhibits a mononuclear structure composed of one acetate anion and one [Cu(HL)(CH_3CH_2OH)]$^+$ cation, [Zn_3(HL1)$_2$(CH_3COO)$_4$] exhibits a trinuclear structure composed of two ZnN_2O_3 coordination units and one ZnO_6 coordination unit, and [Zn_2(L2)]·(CH_3COO) is a binuclear complex composed of two ZnN_2O_3 coordination units. Stimulated by the prior studies, the catalytic

* Corresponding author.
E-mail address: kykrliu@163.com (C. Liu).

https://doi.org/10.1016/j.ica.2020.119639
Received 4 March 2020; Received in revised form 29 March 2020; Accepted 29 March 2020
Available online 31 March 2020
0020-1693/

activities of the complexes in the decomposition of H_2O_2 have been investigated. In addition, in order to further investigate their biological activities, the antibacterial activities of the complexes against gram-negative bacteria and gram-positive bacteria were tested.

2. Experimental

2.1. Materials and methods

Analytical grade diethylenetriamine, triethylenetetramine and salicylaldehyde were acquired from Sigma–Aldrich and used as received. All other reagents and solvents were purchased from commercially available sources without any further purification. The six bacteria in the antibacterial test were presented by the school of pharmacy of Anhui medical university. FT-IR spectra were measured by using KBr pellet technique with a FTS-40 spectrophotometer in the region 400–4000 cm^{-1}. ^1H NMR and ^{13}C NMR spectra for analyses of compounds were recorded on a Bruker AM-400 NMR spectrometer in $CDCl_3$ solution. Elemental analyses for C, H and N were carried out on a Vario EL III elemental analyzer.

2.2. Synthesis

2.2.1. Synthesis of H_2L1

To a solution of diethylenetriamine (2.58 mL, 23.95 mmol) in water (40 mL) was added salicylaldehyde (5.00 mL, 47.90 mmol) slowly by a syringe. A biphasic reaction system was formed due to the slight solubility of salicylaldehyde in water. The reaction mixture was stirred at room temperature for 1 h and the color of the solution gradually changed from colorless to deep yellow. After completing the reaction, the organic layer was separated using a separatory funnel and the aqueous layer was extracted with dichloromethane (2 × 15 mL). Then, the organic fractions were combined and washed with water (2 × 10 mL) and n-hexane (2 × 10 mL), respectively. Removal of the residual solvents gave a yellow oily product H_2L1. Yield: 92%. Anal. Calcd for $C_{18}H_{21}N_3O_2$ (%): C, 69.43; H, 6.80; N, 13.49. Found: C, 69.41; H, 7.08; N, 13.28. ^1H NMR (400 MHz, $CDCl_3$): δ = 13.37 (br, 2H, OH), 8.35 (s, 2H, N = CH), 7.30–6.83 (m, 8H, Ar-H), 3.71 (t, 4H, C = NCH_2), 3.00 (s, 4H, CH_2NHCH_2). ^{13}C NMR (100 MHz, $CDCl_3$): δ = 166.1, 161.1, 132.3, 131.3, 118.7, 118.6, 117.0, 59.5, 49.7.

2.2.2. Synthesis of H_3L2

The compound was prepared as a yellow solid in 88% yield by the treatment of triethylenetetramine (2.38 mL, 15.97 mmol) with salicylaldehyde (5.00 mL, 47.90 mmol) in 40 mL of water using the similar procedure for the preparation of H_2L1. Anal. Calcd for $C_{27}H_{30}N_4O_3$ (%): C, 70.72; H, 6.59; N, 12.22. Found: C, 70.89; H, 6.64; N, 11.96. ^1H NMR (400 MHz, $CDCl_3$): δ = 13.18 (br, 2H, OH), 10.61 (br, 1H, OH), 8.25 (s, 2H, N = CH), 7.30–6.78 (m, 12H, Ar-H), 3.84 (s, 1H, NCHN), 3.59 (t, 4H, C = NCH_2), 2.97 (t, 4H, C = NCH_2CH_2), 2.67 (t, 4H, NCH_2CH_2N). ^{13}C NMR (100 MHz, $CDCl_3$): δ = 166.0, 161.1, 158.2, 132.2, 131.4, 130.9, 130.2, 120.8, 118.7, 118.5, 117.0, 89.6, 58.5, 52.8, 51.2.

2.2.3. Synthesis of $[Cu(HL1)(CH_3CH_2OH)]\cdot(CH_3COO)$ (1)

To a solution of $Cu(OAc)_2\cdot H_2O$ (0.74 g, 3.71 mmol) in ethanol (30 mL) was added an ethanol solution of H_2L1 (1.00 mL, 3.71 mmol) at room temperature. The reaction mixture was stirred under reflux for 20 h and then filtered off after being cooled to room temperature. The filtrate was evaporated to dryness under reduced pressure to provide a dark blue residue. The residue was dissolved in a co-solvent of ethanol and dichloromethane (v: v = 1: 1) and blue single crystals of **1** were obtained at room temperature after 48 h. Yield: 71%, m.p. 115.0–116.5 °C. Anal. Calcd for $C_{22}H_{28}N_3O_5Cu$ (%): C, 55.28; H, 5.90; N, 8.79. Found: C, 55.47; H, 6.15; N, 8.65. IR (KBr, cm^{-1}): 3443(vs), 3142(m), 2928(s), 2573(m), 2388(m), 1635(s), 1597(s), 1553(vs), 1449(s), 1307(m), 1247(m), 1148(m), 1050(m), 919(m), 864(w), 766(s), 706(m), 640(w), 608(w), 520(w).

2.2.4. Synthesis of $[Zn_3(HL1)_2(CH_3COO)_4]$ (2)

The complex was prepared as a white crystal in 83% yield by the treatment of $Zn(OAc)_2\cdot 2H_2O$ (1.22 g, 5.57 mmol) with H_2L1 (1.00 mL, 3.71 mmol) in 40 mL of ethanol using the similar procedure for the preparation of complex **1**. m.p. 172.5–174.0 °C. Anal. Calcd for $C_{44}H_{50}N_6O_{12}Zn_3$ (%): C, 50.28; H, 4.79; N, 8.00. Found: C, 50.24; H, 5.01; N, 7.95. IR (KBr, cm^{-1}): 3431(m), 3224(s), 2924(s), 2853(m), 1646(s), 1575(s), 1471(s), 1443(s), 1416(m), 1307(s), 1187(m), 1154(w), 1127(m), 1039(m), 1006(m), 897(w), 826(w),750(s), 662(m), 602(w), 531(w).

2.2.5. Synthesis of $[Zn_2(L2)]\cdot(CH_3COO)$ (3)

The complex was prepared as a white crystal in 79% yield by the treatment of $Zn(OAc)_2\cdot 2H_2O$ (0.96 g, 4.36 mmol) with H_3L2 (1.00 g, 2.18 mmol) in 40 mL of ethanol using the similar procedure for the preparation of complex **1**. m.p. 197.0–199.5 °C. Anal. Calcd for $C_{29}H_{30}N_4O_5Zn_2$ (%): C, 53.97; H, 4.69; N, 8.68. Found: C, 53.73; H, 4.95; N, 8.70. IR (KBr, cm^{-1}): 3471(s), 3325(s) 2968(m), 1635(s), 1553(s), 1449(s), 1411(s), 1339(m), 1312(m), 1258(m), 1252(m), 1191(m), 1148(s), 1022(m), 919(m), 853(w), 750(m),711(w), 679(m), 609(w).

2.3. Crystal structure determination

Single crystals of complexes **1**, **2** and **3** were carefully selected and glued to thin glass fibers. The diffraction data were collected on a Bruker APEX-II CCD diffractometer for complex **2** and a Bruker *P*4 diffractometer for complexes **1** and **3** at 296(2) K equipped with Mo Kα radiation (λ = 0.71073 Å). After data reduction and cell refinement were performed with the SAINT program, a multi-scan empirical absorption correction was applied to the data by using the SADABS program [27]. The crystal structures were solved by direct methods and refined by full-matrix least-squares on F^2 using SHELXL-97 [28] for complex **2** and SHELXL-2018/3 [29] for complexes **1** and **3**. All non-hydrogen atoms were refined by anisotropic thermal parameters. The hydrogen atoms were set in calculated positions and the isotropic thermal parameters were fixed during the structure refinement. The crystallographic data and structure refinement parameters of complexes **1**, **2** and **3** are summarized in Table 1, the selected bond lengths and angles are listed in Table S1, and the hydrogen bonding parameters are summarized in Table S2. CCDC: 1585125, complex **1**; 1585124, complex **2**; 1585126, complex **3**.

2.4. General procedure for decomposition of hydrogen peroxide [30]

To a 50 mL round-bottom flask was added the synthesized compound (1.0 mmol) and DMF (5 mL), and then an aqueous solution of H_2O_2 (20 mL, 15 wt%) was carefully injected into the solution by a syringe. The reaction was carried out at room temperature for 24 h. After completing the reaction, the residual concentration of H_2O_2 was titrated with a $KMnO_4$ standard solution and the decomposition percent of H_2O_2 was further calculated.

2.5. Biological activity assay

All the synthesized ligands and complexes have been screened for their antibacterial activities *in vitro*. Three gram-negative bacteria including *Escherichia coli* (ATCC 25922), *Klebsiella pneumoniae* (ATCC 70063) and *Pseudomonas aeruginosa* (ATCC 27853) and three gram-positive bacteria including *Bacillus subtilis* (ATCC 6633), *Staphylococcus aureus* (ATCC 25923) and *Corynebacterium xerosis* (ATCC 373) were used as the test microorganisms.

The primary screening was carried out by the disc diffusion method [31]. Dimethylsulphoxide (DMSO) with no inhibiting effects on the

Table 1
Crystallographic data and structure refinement parameters for complexes **1**, **2** and **3**.

Complex	1	2	3
Formula	$C_{22}H_{29}N_3O_5Cu$	$C_{44}H_{50}N_6O_{12}Zn_3$	$C_{29}H_{30}N_4O_5Zn_2$
Fw	479.03	1051.07	645.31
Temperature	296(2)	296(2)	296(2)
Crystal system	Monoclinic	Tetragonal	Triclinic
Space group	*Cc*	$I4_1/a$	*P*$\bar{1}$
a (Å)	16.6146(16)	24.454(6)	10.144(2)
b (Å)	7.5227(7)	24.454(6)	11.501(2)
c (Å)	18.9472(17)	16.024(4)	16.118(3)
α	90.00	90.00	91.97(3)
β	101.911(3)	90.00	93.83(3)
γ	90.00	90.00	110.58(3)
Volume (Å^3)	2317.2(4)	9582(4)	1753.1(7)
Z	4	8	2
Dcalcd/(g·cm^{-3})	1.370	1.457	1.223
μ (mm^{-1})	0.979	1.555	1.405
F (0 0 0)	1004	4336	664
Crystal size (mm)	0.22 × 0.25 × 0.28	0.22 × 0.25 × 0.27	0.11 × 0.12 × 0.13
Reflections collected	7772	26,223	16,272
Unique reflections (R_{int})	3203 (0.025)	4221 (0.048)	8577(0.025)
Gof	1.055	1.034	1.040
Final *R* indices [*I* > 2*σ*(*I*)]	R_1 = 0.0320, wR_2 = 0.0813	R_1 = 0.0318, wR_2 = 0.0729	R_1 = 0.0374, wR_2 = 0.1006
R indices (all data)	R_1 = 0.0351, wR_2 = 0.0833	R_1 = 0.0554, wR_2 = 0.0843	R_1 = 0.0515, wR_2 = 0.1063
Largest diff. peak and hole (e Å^{-3})	0.44 and −0.31	0.43 and −0.18	0.37 and −0.53

[a]$R = \Sigma(||F_o| - |F_c||)/\Sigma|F_o|$, [b]$wR = [\Sigma w(|F_o|^2 - |F_c|^2)^2/\Sigma w(F_o^2)]^{1/2}$.

microorganisms was used as solvent to dissolve the compounds. The standard drugs, ciprofloxacin (for gram-positive) and gentamicin (for gram-negative), were used as positive references. The discs (diameter 6 mm) impregnated separately with the compounds at the concentration of 10 mg/mL were placed on the inoculated agar plates and all the plates were incubated at 37 °C for 24 h. By measuring the inhibition zone diameters, the antibacterial activities were evaluated and recorded. The secondary screening was carried out by measuring the minimum inhibitory concentration (MIC). The compounds were dissolved in DMSO to prepare the solutions with the initial concentration of 256 μg/mL, whose final concentration ranged from 256 to 0.5 μg/mL with two-fold serial dilutions. A standard suspension of the microorganism was diluted in broth media to obtain a final concentration of 1×10^6 colony-forming units(CFU)/mL. The sterile micro plates were incubated for 24 h at 37 °C for all bacteria strains. MIC was the lowest antibacterial concentration and chosen as the evaluation criterion. All the assays were repeated in triplicate.

3. Results and discussion

3.1. Synthesis of the ligands and the complexes

The ligands H_2L1 and H_3L2 have been synthesized by the condensation of salicylaldehyde with diethylenetriamine (2:1 M ratio) and triethylenetetramine (3:1 M ratio) in water (Scheme 1). H_2L1 and H_3L2 were obtained as a yellow oil in 92% yield and a yellow solid in 88% yield, respectively. The purity and structure of the ligands were authenticated by elemental analyses and NMR spectroscopy. Compared with the similar compounds synthesized in organic solvents [32,33], these ligands could be prepared more effectively by using water as solvent at room temperature.

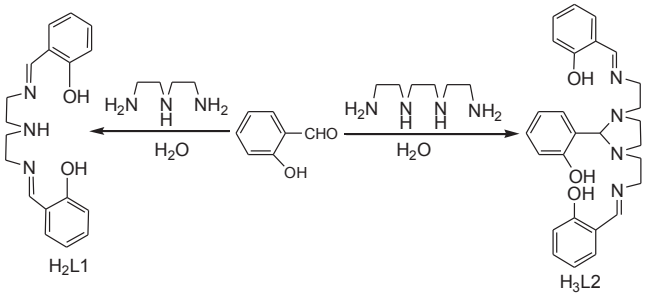

Scheme 1. Synthesis of the ligands.

Complexes **1** and **2** have been synthesized by the reactions of H_2L1 with $Cu(OAc)_2{\cdot}H_2O$ (1:1 M ratio) and $Zn(OAc)_2{\cdot}2H_2O$ (2:3 M ratio) under refluxing, respectively (Fig. 1 and Fig. 2). Moreover, we also tried to synthesize the other two Cu(II) and Zn(II) complexes by the reactions of H_3L2 with $Cu(OAc)_2{\cdot}H_2O$ and $Zn(OAc)_2{\cdot}2H_2O$, respectively. But unfortunately, only complex **3** has been synthesized as a white crystal in 79% yield (Fig. 3), the copper complex hasn't been obtained under the same conditions [1–45]. By summarizing the preparation of the Cu(II) and Zn(II) complexes with similar ligands [34], we would try to synthesize the copper complex using different methods in the following study. The complexes were stable in air and were fully characterized by IR, melting point, elemental analyses, and single crystal X-ray diffraction.

3.2. Structure description

3.2.1. Structure of complex 1

The results of the single crystal X-ray diffraction analysis reveal that the asymmetric unit of complex **1** contains one acetate anion and one

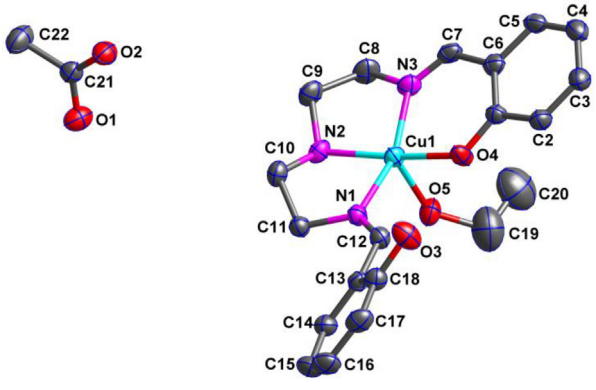

Fig. 1. Crystal structure of complex **1** with 30% probability ellipsoids (H atoms are omitted for clarity).

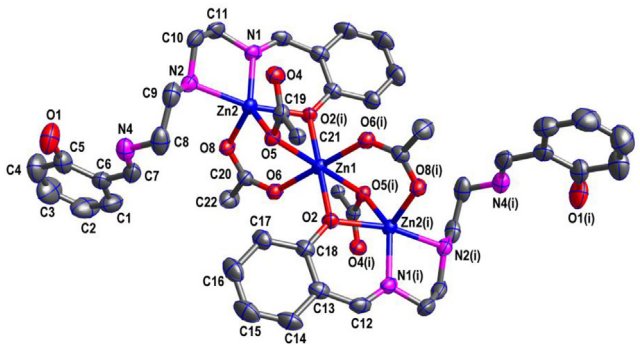

Fig. 2. Crystal structure of complex **2** with 30% probability ellipsoids (H atoms are omitted for clarity). Symmetry code: (*i*) 2 − x, −y, −z.

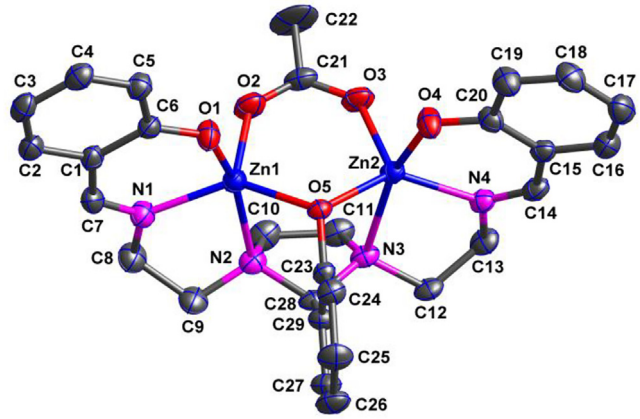

Fig. 3. Crystal structure of complex **3** with 30% probability ellipsoids (H atoms are omitted for clarity).

mononuclear $[Cu(HL)(CH_3CH_2OH)]^+$ cation, which crystallizes in monoclinic crystal system with *Cc* space group. The crystal structure of complex **1** is shown in Fig. 1. The Cu(II) ion is coordinated by an ethanol molecule in an η^1 mode and a deprotonated N_3O Schiff base ligand in an η^4 mode, resulting in a slightly distorted square-pyramidal CuN_3O_2 coordination geometry. The τ value is applicable to the penta-coordinated structure as an important index of the degree of trigonality [35], which helps us distinguish the square pyramidal geometry. The central Cu1 ion, with trigonality index τ = 0.206 which deviates from 0 (ideal square pyramid) and 1 (ideal trigonal bipyramid), is situated in a distorted square pyramidal environment. The basal plane consists of one hydroxyl oxygen atom (O4), two imino nitrogen atoms (N1 and N3) and one secondary amine nitrogen atom (N2) from the ligand. The axial position is occupied by one oxygen atom (O5) from the ethanol molecule. The Cu1—N1, Cu1—N2, and Cu—N3 bond distances are 1.990(5), 2.010(5) and 1.936(5)Å, respectively, which are in agreement with those of the reported structures [36,37]. The Cu1—O5 bond (2.323(3) Å) is significantly longer than the Cu1—O4 bond (1.906(4) Å), which indicates that the strength of the Cu1—O5 bond is weaker than that of the Cu1—O4 bond. The bond angles N1—Cu1—N2 (84.28(19)°), N2—Cu1—N3 (85.1(2)°), O4—Cu1—N3 (93.8(2)°) and O4—Cu1—N1 (94.59(18)°) are added up to 357.77° unequal to 360°. The bond angles O5—Cu1—N1 (99.03(18)°), O5—Cu1—N2 (91.78(17)°), O5—Cu1—N3 (97.65(18)°) and O4—Cu1—O5 (95.91(16)°) are all different to the ideal value of 90°. All those indicate that the central Cu1 ion adopts a distorted square pyramidal geometry. Furthermore, there is one acetate anion in the asymmetric unit, which acts as the counter anion to balance the valence charge of the $[Cu(HL)(CH_3CH_2OH)]^+$ cation. There exist three types of intermolecular hydrogen bonds (N2—H2A…O1(*i*), O3—H3A…O1(*ii*) and O5—H5A…O2(*i*)) and four types of nonclassical hydrogen bonds (C9—H9A…O2(*iii*), C10—H10B…O2(*iii*), C12—H12…O4 and C16—H16…O2(*iv*)). Under the weak interactions, the crystal structure is further stabilized. The crystal packing diagram of complex **1** is shown in Fig. S1.

3.2.2. Structure of complex 2

Complex **2** is a bridged trinuclear Zn(II) molecule, which crystallizes in tetragonal crystal system with $I4_1/a$ space group. As shown in Fig. 2, the asymmetric unit consists of only half of the molecule, which contains three crystallographically independent Zn(II) cations, two deprotonated N_2O Schiff base ligands and four acetates. Zn2 ion has the same coordination environment with Zn2(i) ion, where Zn2 ion is penta-coordinated by one oxygen atom (O2(i)) and two nitrogen atoms (N1 and N2) from one tridentate chelating H_2L1 ligand, one bridging oxygen atom (O5) from one monodentate acetate, and one oxygen atom (O8) from one bidentate bridging acetate, exhibiting a slightly distorted trigonal bipyramidal ZnN_2O_3 coordination geometry. The three atoms (O5, O8 and N1) define the basal plane of the trigonal bipyramidal structure, while N2 and O2(i) atoms are located in the axial position with the N2—Zn2—O2(i) angle of 167.84(9)°. The Zn2—N bond distances are in the ranges of 2.022(3) and 2.184(3) Å and the Zn2—O bond distances are in the ranges of 1.992(2) and 2.144(2) Å, which are similar to those in other related Zn(II) complexes [38,39]. The sum of the bond angles O5—Zn2—O8 (104.58(8)°), O5—Zn2—N1 (140.16(10)°) and O8—Zn2—N1 (113.87(10)°) around the metal center is 358.61°, which further confirms that the four atoms are nearly coplanar. Zn1 ion is six-coordinated by two oxygen atoms (O6 and O6(i)) from two bidentate bridging acetates, two bridging oxygen atoms (O5 and O5(i)) from two monodentate acetates, and two bridging hydroxyl oxygen atoms (O2 and O2(i)) from two H_2L1 ligands. A slightly distorted octahedral ZnO_6 coordination structure is observed in the Zn1 ion, with two hydroxyl oxygen atoms (O6 and O6(i)) in the axial position and four oxygen atoms (O2, O5, O2(i) and O5(i)) from four acetates in the equatorial plane. The Zn1—O bond lengths fall in the ranges of 2.054(2) and 2.2168(19)Å, while the bond angles around Zn1 ion fall in the ranges of 79.72(7) ° and 100.28(7)°. Zn1 ion affords a bridged trinuclear Zn_3 building subunit together with the Zn2 ion and its symmetric Zn2(i) ion. The adjacent Zn(II) ions (Zn1, Zn2 and Zn2(i)) are bridged by two acetates in a μ_2-η^1:η^1-bridging coordination mode, two acetates in a μ_2-η^2-bridging mode, and two H_2L1 ligands in a μ_2-η^1:η^1:η^2-chelating/bridging mode, with a nonbonding Zn1…Zn2 distance of 3.0571(6) A°. As shown in Fig. S2, one intramolecular hydrogen bond (O1—H1…N4) and three types of nonclassical hydrogen bonds (C9—H9A…O4, C11—H11B…O4(*ii*) and C17—H17…O5) are also observed in complex **2**. By the hydrogen bond interactions, the complex molecules are extended into an infinite 3D supramolecular framework structure.

3.2.3. Structure of complex 3

Complex **3** is a bridged binuclear Zn(II) molecule, which crystallizes in triclinic crystal system with $P\bar{1}$ space group. As shown in Fig. 3, the asymmetric unit of complex **3** contains two crystallographically independent Zn(II) cations, one deprotonated N_4O_3 Schiff base ligand and one acetate. Zn1 ion has the same coordination environment with Zn2 ion, where Zn1 is penta-coordinated by two oxygen atoms (O1 and O5) and two nitrogen atoms (N1 and N2) from one seven-dentate chelating H_3L2 ligand, and one oxygen atom (O2) from one bidentate bridging acetate, exhibiting a slightly distorted trigonal bipyramidal ZnN_2O_3 coordination geometry. The basal plane is defined by one hydroxyl oxygen atom (O5), one imino nitrogen atoms (N1) and one oxygen atom (O2), while the axial position is occupied by one secondary amine nitrogen atom (N2) and one hydroxyl oxygen atom (O1) with the O1—Zn1—N2 angle of 162.63(8)°. The Zn—N bond distances range from 2.014(2) to 2.406(2) A° and the Zn—O bond distances are in the ranges of 1.9795(19) and 1.9945(19) Å. The bond angles O5—Zn1—N1 (139.15(8)°), O2—Zn1—O5 (109.38(8)°) and O2—Zn1—N1 (109.73(9)°) around the metal center are added up to 358.26°,

Table 2
Optimization of decomposition conditions of hydrogen peroxide.

Entry	Catalyst	Catalyst loading (mmol)	Decomposition percent (%)
1	Complex **1**	0.1	17
2		0.5	59
3		1.0	97
4		1.5	97
5		2.0	98
6	Complex **2**	0.1	25
7		0.5	47
8		1.0	93
9		1.5	93
10		2.0	93
11	Complex **3**	0.1	21
12		0.5	52
13		1.0	89
14		1.5	91
15		2.0	92
16	H_2L1	1.0	0
17	H_3L2	1.0	0
18	$Cu(OAc)_2{\cdot}H_2O$	1.0	60
19	$Zn(OAc)_2{\cdot}2H_2O$	1.0	74

approximately equal to 360°, indicating that Zn1 ion is nearly coplanar with the three coordination atoms. Interestingly, it is observed that there exist two kinds of different coordination modes for the hydroxyl oxygen atoms from the ligand. One hydroxyl oxygen atom (O1) is only coordinated to Zn1 ion in an η^1 mode, while the other hydroxyl oxygen atom (O5) is coordinated to both Zn1 and Zn2 ions in a μ_2-η^1:η^1-bridging mode. Zn2 ion affords a binuclear Zn_2 building subunit together with the Zn1 ion. The adjacent Zn(II) ions (Zn1 and Zn2) are bridged by one bidentate acetate and one hydroxyl oxygen atoms (O3) from the ligand, with a nonbonding Zn1…Zn2 distance of 3.2293(11) A°. Unlike complexes **1** and **2**, there exist no hydrogen bonds in complex **3**. The crystal packing diagram of complex **3** is shown in Fig. S3.

3.3. Catalytic activity

Hydrogen peroxide, a typical inorganic reductant and oxidant, could be decomposed with some suitable transition metal compounds as catalyst [40,41]. In order to investigate the catalytic activities of the synthesized compounds, the catalytic decomposition of H_2O_2 was examined at room temperature.

As shown in Table 2, there is a close relationship between the decomposition percent of H_2O_2 and the catalyst loading. In the presence of complex **1** as catalyst, the decomposition reaction of H_2O_2 could be carried out well. When the catalyst loading was below 1.0 mmol, the decomposition percent increased significantly with the increasing of the catalyst loading (Table 2, entries 1–3). Increasing the catalyst loading to 1.0 mmol, the decomposition percent reached up to 97%. When the catalyst loading was beyond 1.0 mmol (Table 2, entries 4–5), the decomposition percent remained almost constant. In the meantime, the catalytic activities of complexes **2** and **3** were also surveyed. The results showed that the catalytic reaction could be performed efficiently with a catalyst loading ranging between 1.0 and 2.0 mmol (Table 2, entries 8–10, 13–15). It is interesting to find that when the loading of complexes **2** and **3** was 1.0 mmol equal to that of complex **1**, the decomposition percents of 93% and 89% have been obtained, respectively (Table 2, entries 8 and 13). Further increase in the catalyst loading did not improve the catalytic activities of complexes **2** and **3** appreciably. In consideration of the decomposition percent and the cost of catalyst, a catalyst loading of 1.0 mmol is the most suitable for the decomposition reaction. Additionally, the two ligands were used to catalyze the decomposition of H_2O_2. But unfortunately, the residual concentration of H_2O_2 remained virtually unchanged, which indicated that the ligands showed poor catalytic activities (Table 2, entries 16–17). The decomposition reaction could also be catalyzed by some acetates such as $Cu(OAc)_2{\cdot}H_2O$ and $Zn(OAc)_2{\cdot}2H_2O$ [30,42]. The results of the literatures showed that the decomposition percents only reached 60% and 74% with equal amount of $Cu(OAc)_2{\cdot}H_2O$ and $Zn(OAc)_2{\cdot}2H_2O$ as catalyst (Table 2, entries 18–19). Compared to $Cu(OAc)_2{\cdot}H_2O$ and $Zn(OAc)_2{\cdot}2H_2O$, our complexes showed better catalytic activities in the decomposition of H_2O_2, which has a certain practical significance for the development of new efficient catalysts.

Taking into account of the above finding and the metal content in catalyst, complex **1** was chosen as the catalyst for the decomposition reaction of H_2O_2.

3.4. Antibacterial activity

Copper and zinc complexes have a wide range of biological activities, especially in antibacterial activities, so in order to investigate the biological activities of the complexes, their antibacterial activities against gram-negative bacteria and gram-positive bacteria were screened. For the primary screening, the inhibition zone diameters were tested and the results were presented in Table 3. The two Schiff base ligands exhibited very weak activities against the bacteria and the solvent DMSO had no inhibiting effects. Compared to the two ligands, complexes **1**, **2** and **3** had larger bacterial inhibition zones. Complex **1** exhibited stronger antibacterial activities against *S. aureus* with an inhibition zone diameter of 14 mm than other five bacteria with inhibition zone diameters between 11 mm and 13 mm. In addition, complex **2** exhibited excellent inhibitory activities against *K. pneumoniae* with an inhibition zone diameter of 17 mm, while complex **3** exhibited stronger activities against *S. aureus* and *C. xerosis* with an inhibition zone diameter of 14 mm, respectively.

After above primary screening, the MIC values of the compounds were also measured, and two standard drugs (ciprofloxacin and gentamicin) were used as the positive controls (listed in Table 4). Complexes **1**, **2** and **3** showed antibacterial activities against the six bacteria, with the MIC values between 16 and 128 μg/mL, while the MIC values of the ligands were all beyond 128 μg/mL, confirming their poor activities. The antibacterial activities of complexes might be related to the chelation and the biological function of the metal ion, which could be explained by Tweedy's chelation theory [43]. Chelation reduces the

Table 3
Inhibition zone diameter of the ligands, complexes **1**, **2** and **3** and the standard drugs.

Compound	Inhibition zone diameter (mm)					
	B. subtilis	*S. aureus*	*C. xerosis*	*E. coli*	*K. pneumoniae*	*P. aeruginosa*
DMSO	–	–	–	–	–	–
H_2L1	8	7	8	7	8	8
H_3L2	8	9	9	7	8	10
Complex **1**	13	14	13	12	11	12
Complex **2**	14	16	15	15	17	15
Complex **3**	13	14	14	12	13	12
Ciprofloxacin	23	28	27	–	–	–
Gentamicin	–	–	–	25	25	27

Table 4
MIC of the ligands, complexes **1**, **2** and **3** and the standard drugs.

Compound	MIC (μg/mL)					
	B. subtilis	*S. aureus*	*C. xerosis*	*E. coli*	*K. pneumoniae*	*P. aeruginosa*
H_2L1	256	> 256	256	> 256	> 256	256
H_3L2	256	128	256	> 256	256	256
Complex **1**	64	32	64	128	128	128
Complex **2**	64	16	32	64	16	64
Complex **3**	128	32	64	128	64	128
Ciprofloxacin	1.0	0.5	1.0	–	–	–
Gentamicin	–	–	–	0.5	2.0	1.0

polarity of the metal ion because the positive charge of the ion is partially shared by the donor groups of the ligand, and then the abilities of complexes to cross cell membranes are enhanced. The MIC value of complex **1** against the gram-positive bacteria *S. aureus* was 32 μg/mL and those against two other gram-positive bacteria were both 64 μg/mL. Interestingly, it could be observed that complex **1** showed antibacterial activities against the three gram-negative bacteria with the same MIC value of 128 μg/mL. The MIC values of complex **2** were observed between 16 and 64 μg/mL, while those of complex **3** containing the same Zn(II) ion were between 32 and 128 μg/mL. In comparison with complex **2**, the MIC values of complex **3** increased two-fold to four-fold against the same bacteria, respectively. The strong antibacterial activities of complex **2** may be mainly due to two factors. On the one hand, complex **2** exhibits a trinuclear Zn_3 molecule structure, while complex **3** is a binuclear Zn_2 molecule. On the other hand, two H_2L1 ligands exist in complex **2**, while only one H_3L2 ligand exists in complex **3**. According to the relevant literatures as well as the membrane theory of cell permeability [44,45], the special structure of complex **2** is more beneficial for its penetration through the cell membranes. Compared with ciprofloxacin and gentamicin, complex **2** showed slightly weaker antibacterial activities against the tested bacteria.

4. Conclusion

In summary, three copper(II) and zinc(II) complexes bearing salicylaldehyde-imine ligands have been designed and synthesized under solvothermal conditions. Complex **1** exhibits a mononuclear structure, which contains one acetate anion and one mononuclear $[Cu(HL)(CH_3CH_2OH)]^+$ cation. Complex **2** is composed of two ZnN_2O_3 coordination units and one ZnO_6 coordination unit, which are further linked into a trinuclear Zn_3 molecule structure by four acetates and two H_2L1 ligands. Complex **3** is composed of two ZnN_2O_3 coordination units, which are further linked into a binuclear Zn_2 molecule structure by one acetate and one H_3L2 ligand.

The results of their catalytic activities indicated that the complexes could efficiently catalyze the decomposition reaction of H_2O_2, while the two Schiff base ligands had no catalytic effects. Compared to complexes **2** and **3**, complex **1** exhibited higher catalytic activities in the decomposition reaction. In addition, the results of structure–activity relationship showed that the complexes had stronger antibacterial activities *in vitro* than the ligands and that complex **2** with the MIC values ranging from 16 to 64 μg/mL had stronger antibacterial activities than complexes **1** and **3**.

CRediT authorship contribution statement

Chao Liu: Conceptualization, Methodology, Resources, Writing - original draft, Supervision. **Ming-Xing Chen:** Validation, Data curation, Resources, Formal analysis. **Ming Li:** Visualization, Investigation, Writing - review & editing.

Declaration of Competing Interest

The authors declare that they have no known competing financial interests or personal relationships that could have appeared to influence the work reported in this paper.

Acknowledgments

This work was supported by the National Natural Science Foundation of China (no. 21977001) and Innovative Research Team of Anhui Provincial Education Department (2016SCXPTTD).

Appendix A. Supplementary data

CCDC 1585125, 1585124 and 1585126 contain the supplementary crystallographic data for complexes **1**, **2** and **3**. These data can be obtained free of charge via http://www.ccdc.cam.ac.uk/conts/retrieving.html or from Cambridge Crystallographic Data Centre, 12 Union Road, Cambridge CB2 1E2, UK; fax:(+44) 1223-336-033; or E-mail: deposit@ccdc.cam.ac.uk. Supplementary data to this article can be found online at https://doi.org/10.1016/j.ica.2020.119639.

References

[1] Y.H. Lin, H.H. Cramer, M.V. Gastel, Y.H. Tsai, C.Y. Chu, T.S. Kuo, I.R. Lee, S. Ye, E. Bill, W.Z. Lee, Inorg. Chem. 58 (2019) 9756–9765, https://doi.org/10.1021/acs.inorgchem.9b00767.
[2] A. Kareem, M.S. Khan, S.A.A. Nami, S.A. Bhat, A.U. Mirza, N. Nishata, J. Mol. Struct. 1167 (2018) 261–273, https://doi.org/10.1016/j.molstruc.2018.05.001.
[3] M. Leist, C. Kerner, L.T. Ghoochany, S. Farsadpour, A. Fizia, J.P. Neu, F. Schön, Y. Sun, B. Oelkers, J. Lang, F. Menges, G.N. Schatteburg, K.S.M. Salih, W.R. Thiel, J. Org. Chem. 863 (2018) 30–43, https://doi.org/10.1016/j.jorganchem.2018.03.022.
[4] K.R. Wilson, D.J. Cannon-Smith, B.P. Burke, O.C. Birdsong, S.J. Archibald, T.J. Hubin, Polyhedron 114 (2016) 118–127, https://doi.org/10.1016/j.poly.2015.11.014.
[5] G. Bauer, X. Hu, Inorg. Chem. Front. 3 (2016) 741–765, https://doi.org/10.1039/C5QI00262A.
[6] B.L. Barreira, J. Díez, P. Crochet, Green Chem. 11 (2009) 1681–1686, https://doi.org/10.1039/b914789f.
[7] M. Khorshidifard, H.A. Rudbari, B. Askari, M. Sahihi, M.R. Farsani, F. Jalilian, G. Bruno, Polyhedron 95 (2015) 1–13, https://doi.org/10.1016/j.poly.2015.03.041.
[8] K. Zhao, Y. Qu, Y.C. Wu, C. Wang, K.S. Shen, C. Li, H.L. Wu, Transit. Met. Chem. 44 (2019) 713–720, https://doi.org/10.1007/s11243-019-00340-4.
[9] A.J. Guwy, A. Farley, P. Cunnah, F.R. Hawkes, D.L. Hawkes, M. Chase, H. Buckland, Water Res. 33 (1999) 3142–3148, https://doi.org/10.1016/S0043-1354(99)00202-X.
[10] H.H. Deng, G.W. Wu, D. He, H.P. Peng, A.L. Liu, X.H. Xia, W. Chen, Analyst 140 (2015) 7650–7656, https://doi.org/10.1039/c5an01284h.
[11] I.A. Salem, M. El-Sheikh, A.B. Zaki, Int. J. Chem. Kinet. 32 (2000) 643–666, https://doi.org/10.1002/chin.200050237.
[12] J.J. Dolhun, J. Chem. Educ. 91 (2014) 760–762, https://doi.org/10.1021/ed4006826.
[13] V.E. Diyuk, V.G. Gerasyova, T.N. Bezuglaya, V.K. Yatsimirskii, Theor. Exp. Chem. 44 (2008) 252–259, https://doi.org/10.1007/s11237-008-9032-y.
[14] S.K. Hai, S.F. Lou, X.Y. Qiu, Chin. J. Inorg. Chem. 32 (2016) 906–912, https://doi.org/10.11862/CJIC.2016.099.
[15] S.S. Jiang, H.H. Ni, F. Liu, S.S. Gu, P. Yu, Y. Gou, Inorg. Chim. Acta 499 (2020) 119186–119192, https://doi.org/10.1016/j.ica.2019.119186.
[16] M. Lavanya, M. Jagadeesh, J. Hari Babu, R. Karvembu, H.K. Rashmi, P.U.M. Devi,

A.V. Reddy, Inorg. Chim. Acta 469 (2017) 76–86, https://doi.org/10.1016/j.ica.2017.08.056.
[17] S. Banerjee, P. Ghorai, P. Sarkar, A. Panja, A. Saha, Inorg. Chim. Acta 499 (2020) 119176–119184, https://doi.org/10.1016/j.ica.2019.119176.
[18] L.D. Chen, H.L. Huo, L.B. Wang, L.L. Ma, Y. Jiang, J.Y. Xie, J. Wang, Chem. Res. Chin. Univ. 34 (2018) 945–951, https://doi.org/10.1007/s40242-018-8186-y.
[19] H.H. Repich, S.I. Orysyk, V.V. Orysyk, Y.L. Zborovskii, V.I. Pekhnyo, M.V. Vovk, J. Mol. Struct. 1144 (2017) 225–236, https://doi.org/10.1016/j.molstruc.2017.05.024.
[20] C. Liu, J.F. Niu, Y. Li, J.G. Xu, X.H. Liu, Chin. J. Struct. Chem. (2016) 1002–1010, https://doi.org/10.14102/j.cnki.0254-5861.2011-1049.
[21] R. Sarkar, A. Hens, K.K. Rajak, RSC Adv. 5 (2015) 15084–15095, https://doi.org/10.1039/c4ra15135f.
[22] A.S. Burlov, S.A. Nikolaevskii, A.S. Bogomyakov, I.S. Vasilchenko, Y.V. Koshchienko, V.G. Vlasenko, A.I. Uraev, D.A. Garnovskii, E.V. Sennikova, G.S. Borodkin, A.D. Garnovskii, V.I. Minkin, Russ. J. Coord. Chem. 35 (2009) 486–491, https://doi.org/10.1134/S1070328409070045.
[23] L. Andrezálová, J. Plšíková, J. Janočková, K. Koňariková, I. Žitňanová, M. Kohútová, M. Kožurková, J. Org. Chem. 827 (2017) 67–77, https://doi.org/10.1016/j.jorganchem.2016.11.007.
[24] O.V. Nesterova, E.N. Chygorin, V.N. Kokozay, V.V. Bon, I.V. Omelchenko, O.V. Shishkin, J. Titiš, R. Boča, A.J.L. Pombeiro, A. Ozarowski, Dalton Trans. 42 (2013) 16909–16919, https://doi.org/10.1039/c3dt51800k.
[25] Y.M. Xu, K. Li, Y.H. Wang, W. Deng, Polymers 9 (2017) 105–114, https://doi.org/10.3390/polym9030105.
[26] E. Pahonțu, D.C. Ilieș, S. Shova, C. Paraschivescu, M. Badea, A. Gulea, T. Roșu, Molecules 20 (2015) 5771–5792, https://doi.org/10.3390/molecules20045771.
[27] G.M. Sheldrick, SADABS: Empirical Absorption Correction Program, University of Göttingen, Göttingen, Germany, 1997.
[28] G.M. Sheldrick, SHELXL-97, Program for Crystal Structure Refinement, University of Göttingen, Germany, 1997.
[29] G.M. Sheldrick, Crystal structure refinement with SHELXL, Acta Crystallogr., C 71 (2015) 3–8, https://doi.org/10.1107/S2053229614024218.
[30] F.Q. Gao, B. Wang, H.Z. Ma, X.N. Yan, Chin. J. Inorg. Chem. 10 (2005) 1460–1464, https://doi.org/10.3321/j.issn:1001-4861.2005.10.004.
[31] K. Siingh, M.S. Barwa, P. Pyagi, Eur. J. Med. Chem. 42 (2007) 394–402, https://doi.org/10.1016/j.ejmech.2006.10.016.
[32] Y.Z. Jiang, Y.Q. Shi, Y.P. Shi, H.Y. Xu, Sci. Sin. 44 (2014) 1528–1535, https://doi.org/10.1360/N032014-00013.
[33] F.R. Xiao, L. Chen, J.D. Wang, R.L. Wu, F. Yue, J. Li, Acta Chim. Sin. 64 (2006) 1517–1522, https://doi.org/10.3321/j.issn:0567-7351.2006.15.001.
[34] P.D. Bernardo, P.L. Zanonato, S. Tamburini, P. Tomasin, P.A. Vigato, Dalton Trans. 39 (2006) 4711–4721, https://doi.org/10.1039/b604211b.
[35] A.Z. Wu, T. Wang, C.C. Zhu, Chin. J. Struct. Chem. 32 (2014) 612–618, https://doi.org/10.1524/zkri.2012.1542.
[36] D.D. Wang, Q.M. Zhu, L. Song, J.Y. Guo, H.Y. Shen, X.R. Wang, W.X. Chai, Polyhedron 175 (2020) 114178–114188, https://doi.org/10.1016/j.poly.2019.114178.
[37] M. Usman, M. Zaki, R.A. Khan, A. Alsalme, RSC Adv. 7 (2017) 36056–36071, https://doi.org/10.1039/c7ra05874h.
[38] X.L. Chen, H.L. Cui, H. Yang, L. Liu, X. Wang, Y.X. Ren, J.J. Wang, B. Han, Chin. J. Struct. Chem. 38 (2019) 2148–2154, https://doi.org/10.14102/j.cnki.0254-5861.2011-2368.
[39] B. Mondal, B. Sen, E. Zangrando, P. Chattopadhyay, J. Chem. Sci. 127 (2015) 1747–1755, https://doi.org/10.1007/s12039-015-0954-3.
[40] K.C. Gupta, H.K. Abdulkadir, S. Chand, J. Appl. Polym. Sci. 90 (2003) 1398–1411, https://doi.org/10.1002/app.12596.
[41] I.A. Salem, M. El-Maazawi, A.B. Zaki, Int. J. Chem. Kinet. 32 (2010) 643–666, https://doi.org/10.1002/chin.200050237.
[42] X.N. Yan, B. Wang, H.Z. Ma, F.Q. Gao, J. Shanxi Normal Univ. 34 (2006) 69–72, https://doi.org/10.3969/j.issn.1672-4291.2006.03.018.
[43] P.K. Panchal, H.M. Parekh, P.B. Pansuriya, M.N. Patel, J. Enzyme Inhib. Med. Chem. 21 (2006) 203–209, https://doi.org/10.1080/14756360500535229.
[44] Q. Al-Awqati, Nat. Cell Biol. 1 (1999) e201–e202, https://doi.org/10.1038/70230.
[45] Q.K. Zhang, C.P. Yue, Y. Zhang, Y.L. Lü, Y.P. Hao, Y.L. Miao, J.P. Li, Z.Y. Liu, Inorg. Chim. Acta 473 (2018) 112–120, https://doi.org/10.1016/j.ica.2017.12.036.